SUMMER SCHOOL AT FERMILAB 2022

ANALYSIS OF THE MUON'S SPIN ANOMALOUS PRECESSION FREQUENCY

DANIELE BOCCANFUSO

Under the supervision of - Brendan Casey, Marco Incagli

Abstract

The muon anomalous magnetic moment, $a_\mu = \frac{g-2}{2}$, is a low energy observable that can be both measured and computed with high precision, thus providing an important test of the Standard Model and a sensitive probe for new physics. The E989 Muon g-2 Experiment at Fermilab aims to measure the muon anomalous magnetic moment to a precision of 140 parts per billion (ppb). The analysis of data from Run 1 led to the result:

$$a_\mu = 116592061 \times 10^{-11} (465 ppb)$$

During my internship at Fermilab I analyzed data from Run 2, estimated the precession frequency ω_a using T and A methods, studied the effect of beam motion dynamics on the result, and estimated the correlation factor between the two methods.

Chapter 1

Muon Magnetic Moment

The muon magnetic moment is given by:

$$\mu = g\frac{q}{2m}\vec{S} \tag{1.1}$$

where q is the particle charge, m is its mass, and g is its giromagnetic factor. The Dirac theory predicts $g = 2$ for any elementary particle of spin $\frac{1}{2}$, as the muon. A small deviation from this value arise from radiative corrections to the Dirac moment (contributions from quantum electrodynamics, electroweak theory, quantum chromodynamics), this additional term increase the value of g by $\mathcal{O}(10^{-3})$, and is called the "anomaly"

$$a_\mu = \frac{g_\mu - 2}{2} \tag{1.2}$$

The anomaly is different for electrons, muons and tauons because of their different masses. Radiative corrections to a_μ receive contributions from all the possible particles coupling to the muon via virtual loops, even hypothetical undiscovered particles, this makes any discrepancy between the theoretical and experimental value of a_μ a hint of new physics.

The measurement is based on the anomalous spin precession frequency of a muon in a magnetic field. For a relativistic particle the frequency at which the particle's momentum changes direction is called cyclotron frequency and is described by the formula:

$$\vec{\omega_c} = -\frac{q}{m\gamma}\vec{B} \tag{1.3}$$

where γ is the Lorentz factor. A particle with spin in a magnetic field experience a torque that causes a precession motion of the particle spin around the direction of the magnetic field,

the precession frequency is given by:

$$\vec{\omega}_s = -g\frac{q}{2m}\vec{B} - (1-\gamma)\frac{q}{m\gamma}\vec{B} \tag{1.4}$$

The anomalous spin precession frequency is defined as:

$$\vec{\omega}_a = \vec{\omega}_s - \vec{\omega}_c = -a_\mu \frac{q}{m}\vec{B} \tag{1.5}$$

This represents the frequency of the particle's spin precession relative to its momentum direction, if g were equal to 2 the spin would always be parallel to the momentum and $\omega_a = 0$. Analysis of the data from Run1 led to the result:

$$a_\mu = 116592040(54) \times 10^{-11} \quad [0.46\,ppm] \tag{1.6}$$

this result combined with the previous measurement from the BNL experiment is the best measurement of the muon anomaly and shows a tension of 4.2σ from the theoretical value. Analysis of successive runs is fundamental to improve the uncertainty on the measurement.

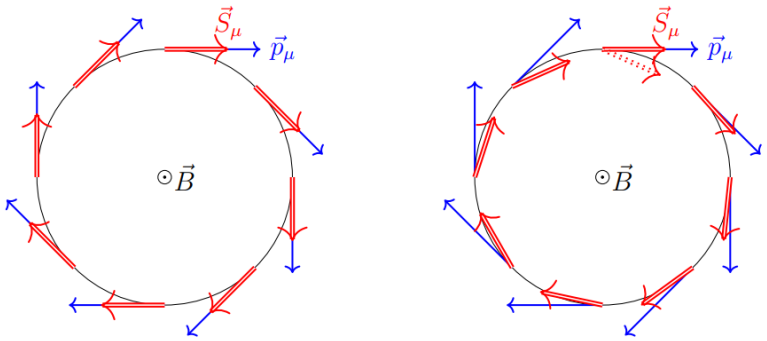

(a) $g = 2$ (b) $g > 2$

Figure 1.1: The blue line represents the momentum direction and the red line represents the spin direction. On the left the case g=2 and on the right the case g>2

Chapter 2

The Experiment

The equation 1.5 is valid for muons with momentum and spin perpendicular to the magnetic field, in the experiment electrostatic quadrupoles are used to confine the muon beam in the storage region and to provide vertical focusing, so the more general equation is:

$$\vec{\omega}_a = \frac{e}{mc}\left[a_\mu \vec{B} - \left(a_\mu - \frac{1}{\gamma^2 - 1}\right)\vec{\beta} \times \vec{E} - a_\mu\left(\frac{\gamma}{\gamma + 1}\right)(\vec{\beta} \cdot \vec{B})\vec{\beta}\right] \tag{2.1}$$

where $\vec{\beta}$ is the muon velocity and $\vec{E}$ is the electric field. The first additional term describes the effect of the electric field and the second the effect of deviations from the ideal orbit. For muons with momentum of $3.094\,GeV$ the correction due to the electric field becomes negligible. Muons decay following the reaction:

$$\mu^+ \rightarrow e^+ \bar{\nu}_\mu \nu_e \tag{2.2}$$

The neutrino and anti-neutrino have opposite helicity and opposite spins, thus the spin of the decay positron must be the same of the muon, in the relativistic limit positrons are righthanded particles, so their spin is parallel to their momentum. This means that high energy positrons emission direction is correlated to muon spin. The number of positrons detected in a fixed direction as a function of time will be modulated by the anomalous precession frequency ω_a. The total number of detected positrons in a fixed direction is described by the following 5 parameters function:

$$N(t) = N_0 e^{-\frac{t}{\gamma\tau}}[1 + A(E)cos(\omega_a t + \phi_0)] \tag{2.3}$$

where N_0 is the number of muons in the beam at $t = 0$, $\gamma\tau$ is the muon lifetime in the

laboratory frame of reference, $A(E)$ is the asymmetry, a function of the positron energy that is tied to the correlation between the positron direction and the muon spin, ω_a is the anomalous precession frequency and ϕ_0 is the initial phase.

2.1 Experiment design

In the Muon g-2 experiment E989, polarized muons are produced from pions decays, pions are produced by 8 GeV protons colliding on a target. The muon beam is injected into a superconducting storage ring, where muons circulate for approximately 750 μs, this time window is called a fill. The superconducting ring produce a vertical magnetic field of $|\vec{B}| \simeq 1.5\,T$, the spin rotates in the plane perpendicular to the magnetic field.

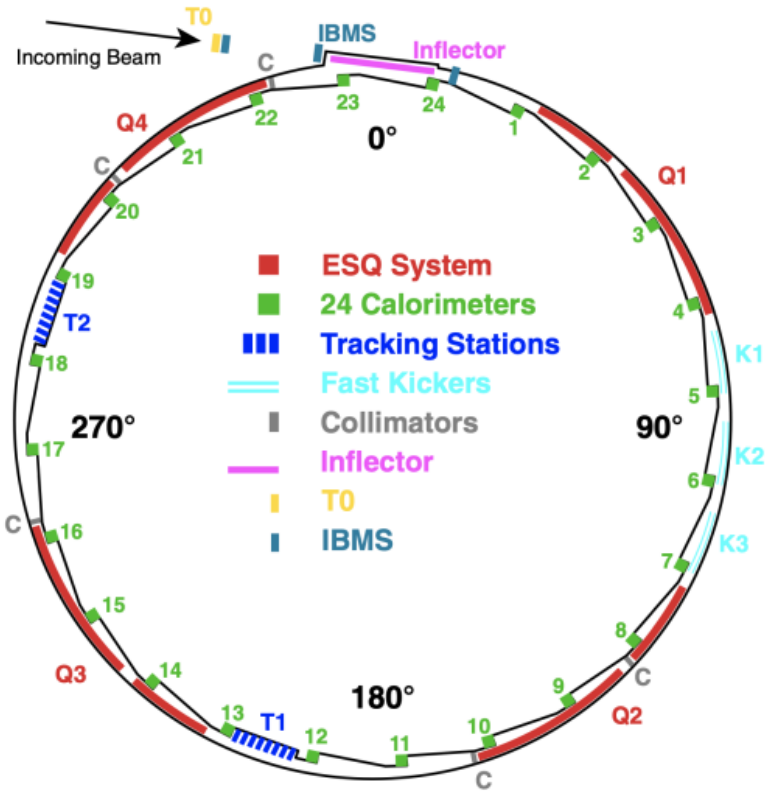

Figure 2.1: Schematics of the above view of the E989 experiment.

The magnetic field in the injection region is nullified by a specific magnet called the inflector, this allows to avoid deflection of the muons before entering the storage region but also causes large particle losses. At this point the muon beam is in an orbit tanget to the storage ring, magnetic kickers produce a strong and short magnetic pulse a the start of every

fill to put the muons in the right orbit. Positrons from dacaying muons curl inward due to the magnetic field, on the inner side of the ring 24 calorimeters are positioned to precisely measure energy and time of arrival of the positrons. Each calorimeter is made of 54 Cerenkov crystals, and as many SiPM for light readout. Two tracker stations, based on drift tubes, are used to reconstruct the beam position by measuring the decay positron trajectories and extrapolating them backward to identify the muon decay vertex. It allows to know the beam distribution as a function of time without affecting the beam itself.

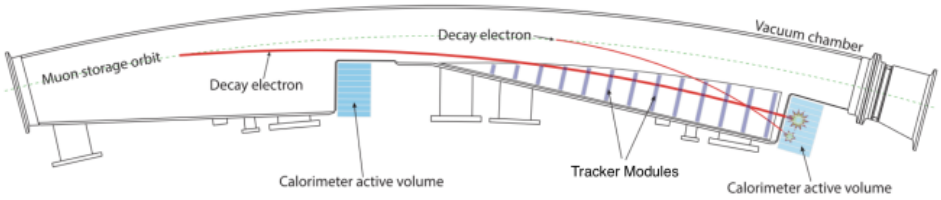

Figure 2.2: Schematics of the section of the storage ring with two calorimeters and a tracker station.

2.2 Beam Dynamics

In the ideal case the beam of muons is in a perfect circular plane orbit, in the real experiment the muon beam moves in the horizontal and vertical directions, known as betatron oscillations, that depend on the machine. In the E989 experiment the vertical magnetic field provides the beam curvature and the horizontal focusing, while the vertical focusing is provided by 4 sets of electrostatic quadrupoles. A quadropole is characterized by a field index n, defined in the following way:

$$n = -\frac{R_0}{\upsilon B_0}\frac{\partial E_y}{\partial y} \tag{2.4}$$

where R_0 is the equilibrium radius, B_0 is the magnetic field, υ the particle speed and E_y the quadropole vertical field. The horizontal and vertical tunes of the machine for a uniform set of quadrupoles are given by:

$$\nu_x = \sqrt{1-n} \tag{2.5}$$

$$\nu_y = \sqrt{n} \tag{2.6}$$

Name	Symbol	Expression
Cyclotron	f_c	$\frac{v}{2\pi R_0}$
Horizontal Betatron	f_x	$\sqrt{1-n}f_c$
Vertical Betatron	f_y	$\sqrt{n}f_c$
Coherent Betatron	f_{CBO}	$f_c - f_x$
Vertical Waist	f_{VW}	$f_c - 2f_y$
Anomalous Precession	f_a	$a_\mu eB/m$

Table 2.1: Table of beam frequencies for n = 0.108

and the corresponding frequencies are:

$$f_x = \sqrt{1-n}f_c \tag{2.7}$$

$$f_y = \sqrt{n}f_c \tag{2.8}$$

where f_c is the cyclotron frequency $\omega_c/2\pi$. Since the field index is directly related to these frequencies, the voltage applied to the electrostatic quadrupole plates has to be carefully chosen in order to avoid beam resonances that would lead to large beam oscillations and to higher particle losses. The beam oscillations introduce a time dependent modulation in the number of detected positrons due to the radial and vertical acceptance of the detectors. The muon bunch, as it rotates in the storage ring, is observed by a fixed detector at the cyclotron frequency fc. As the beam moves on the horizontal plane, since $fx > fc/2$, the frequency observed by each calorimeter is aliased as a coherent betatron oscillation (CBO) of frequency:

$$f_{CBO} = f_c - f_x \tag{2.9}$$

The f_{CBO} is the frequency at which a single calorimeter sees the beam mean position moving coherently in the radial direction. The radial beam width has two oscillation components of frequencies f_{CBO} and $2f_{CBO}$. On the vertical plane there is a similar effect, the beam vertical position oscillates at frequency f_y and the beam vertical width (vertical waist, VW) oscillates at frequency $f_{VW} = f_c - 2f_y$. These betatron oscillation are dumped over time, the decoherence is modeled by a decaying exponential function. An affect that appear as a low frequency oscillations is the effect of lost muons. Lost muons are muons that escape the storage ring before decaying into positrons, mainly due to collisions with collimators.

Chapter 3

Data Analysis

During my internship at Fermilab I analyzed data from Run-2 acquisition period (2019), I analyzed the data using T-method and A-method, which will be explained in details later, observed the impact of beam dynamics effects on the measurement and studied the correlation between the T and A methods with the bootstrap method. As stated in chapter 3.3, the simplest equation that describes the number of positrons detected by the calorimeters as a function of time is 2.3. To avoid cognitive bias, ω_a is blinded by a dimensionless parameter R, defined as the unknown offset in ppm from a reference value. The starting point is reconstructing positrons hits on calorimeters, this can be done using local fitting or global fitting algorithms. From the hit reconstruction energy and time of arrival of the positrons are extracted. When two positrons hit a calorimeter in fast succession the reconstruction algorithm fails to distinguish them and reconstruct them as a single event, these are called Pileup events and are subtracted with a method that will not be discussed in this report.

Figure 3.1 shows the time-energy positrons distribution. The oscillation is already evident at high energy, while is absent at $1000 MeV$, because, as we will see, the asymmetry is zero. We can project this graph on the axes to obtain two important 1D plots. Projecting on the y axis, which means, summing over all entries from a time window, we obtain the energy spectrum. Projecting on the x axis, so summing all entries from a certain energy threshold, we obtain the so called wiggle plot. This projections can be easily done with the method TProjection in ROOT. The wiggle plot is precisely the positron time distribution that we want to fit with an equation like the 2.3. Here this plot is constructed using two different methods.

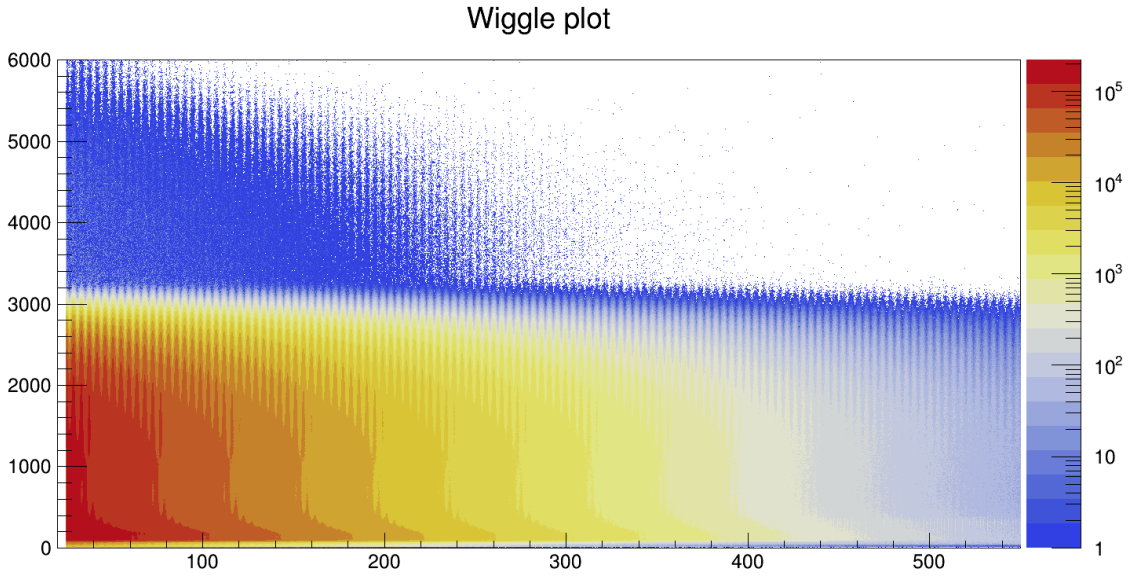

Figure 3.1: Positrons time of arrival (X axis) and energy (Y axis) as measured by the calorimeters. Events above 3.1 GeV are due to Pileup.

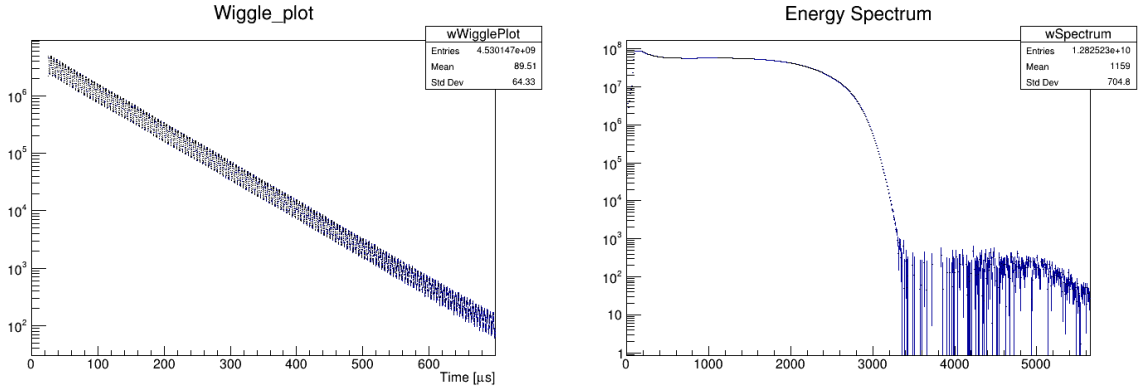

(a) **(b)**

Figure 3.2: (a) wiggle plot (b) energy spectrum

3.1 T-Method

The T-Method consists in building the wiggle plot summing all positrons above an optimal energy threshold. High energy positrons have higher asymmetry and so are more correlated to the muon spin, but as we can see from figure 3.2 (b) the number of positrons rapidly drops near $3.1 GeV$, the majority of positrons have low energy and so less asymmetry. For the integration is necessary to find a energy threshold that compromises between high statistics with low correlation and low statistics with high correlation, the optimal energy threshold is the one that minimizes the error on the parameter R. In order to find the optimal threshold I built 15 wiggle plot changing the low energy threshold each time, than fitted each wiggle plot with the equation 2.3, the plotted the uncertainity on R for every threshold.

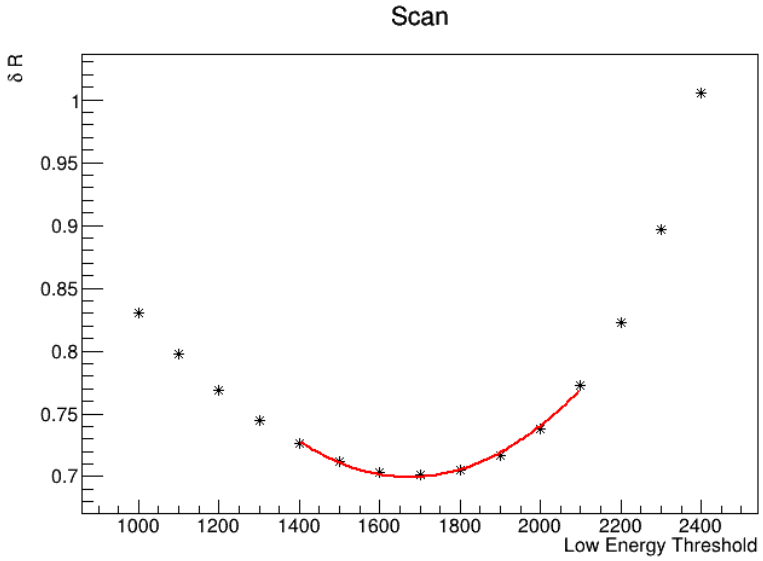

Figure 3.3: Error on R as a function of low energy threshold.

The result of this scan is shown in figure 3.3. This graph is fitted with a quadratic function that has a minimum at $1673 MeV$, this value is close the $1700 MeV$ threshold used in Run-1 analysis. Figure 3.4 shows the result of the fit of the equation 2.3, the parameters are fitted correctly but the χ^2 is still relatively high.

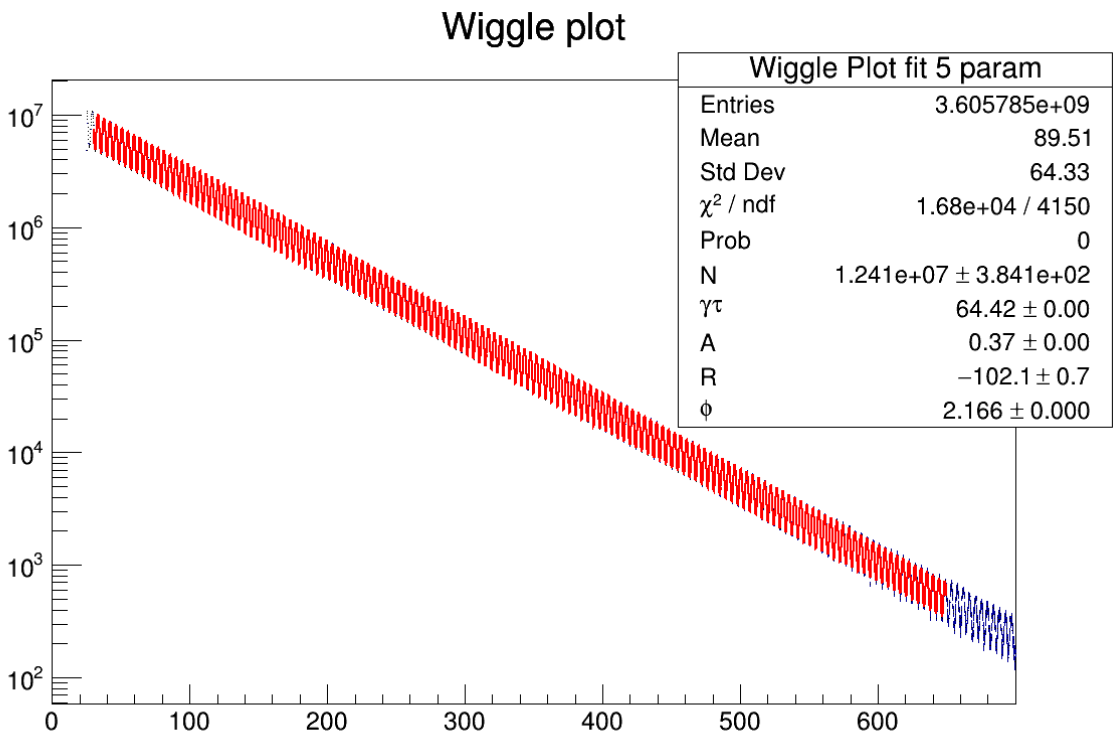

Figure 3.4: Fitted wiggle plot built with the T-Method.

3.2 A-Method

The other method is the A-Method (asymmetry weighted method), in this case each positron is weighted with its asymmetry, which is a function of the energy as stated is section 2. In this way high energy positrons weights more, increasing the sensitivity to the precession frequency signal, low energy positrons weight less so a lower energy threshold can be used. To obtain the asymmetry function, the data region from $500 Mev$ to $3100 Mev$ is sliced in bins

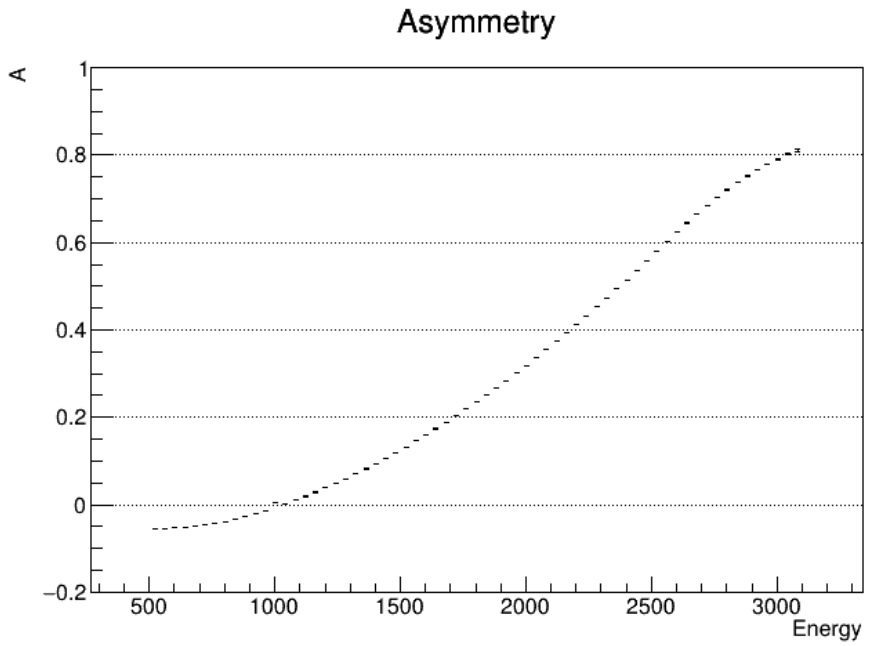

Figure 3.5: Asymmetry as a function of energy, obtained from experimental data with bins of 40 MeV.

of $40 Mev$, each bin is a wiggle plot fitted to extract the asymmetry value. Figure 3.5 shows the result of this operation, as expected the asymmetry is negative for energies below $1000 MeV$ and is monotonically increasing. Finally this graph is interpolated so that is possible to assign a weight for any energy. A weighted wiggle plot is generated integrating from $1100 MeV$, as shown in figure 3.6.

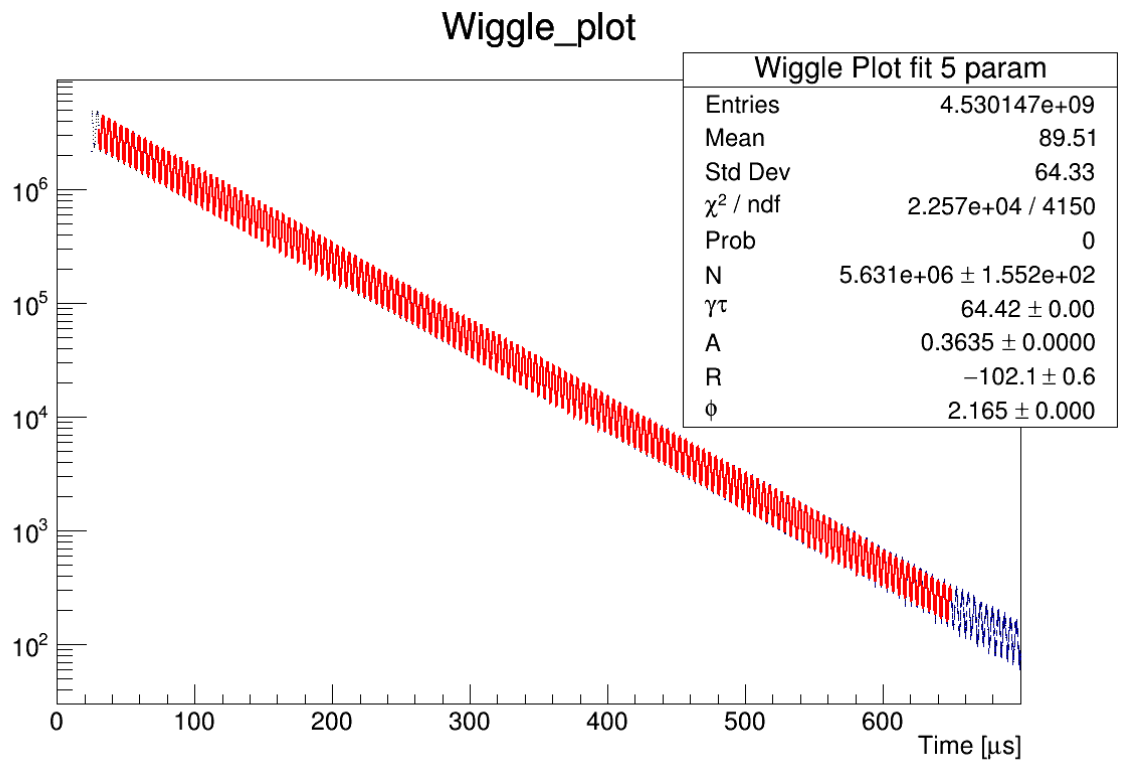

Figure 3.6: Fitted wiggle plot built with the A-method.

3.3 Beam motion effects

In this experiment, effects of beam dynamics have a direct impact on the result. Such effects have already been discussed in section 2. The five parameters fitting function doesn't

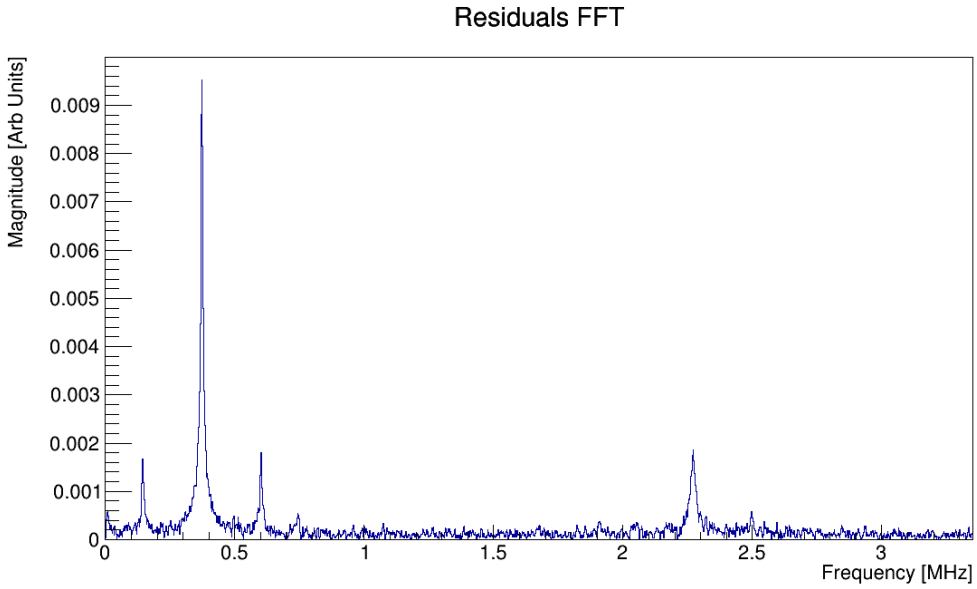

Figure 3.7: Fourier transform of the residuals. The highest peak is the frequency of the CBO, the smaller peaks on the sides are the interference of the CBO withe the precession frequency. The peak on the right is the vertical waist. The small peak a low frequencies is the effect of lost muons.

account for these effects, in fact the Fast Fourier Transform (FFT) of the residuals highlights the frequencies of the beam dynamics oscillations 3.7. The highest peak is the one of the CBO, the oscillation of the beam mean in the horizontal plane. The fittig function must be modified to account for contributions from beam dynamics, this will also improve the fit χ^2. The modified function has 22 parameters and has the following expression:

$$N(t) = N_0 e^{-\frac{t}{\gamma tau}} \left(1 + A_a \cdot A_{BO}(t) cos(\omega_a t + \phi + \phi_{BO}(t))\right) \cdot N_{CBO}(t) \cdot N_{VW}(t) \cdot N_y(t) \cdot N_{2CBO}(t) \cdot \Lambda(t) \tag{3.1}$$

$$
\begin{aligned}
N_{CBO}(t) &= 1 + A_{CBO} cos(\omega_{CBO}(t) + \phi_{CBO}) e^{-\frac{t}{\gamma\tau}} \\
N_{2CBO}(t) &= 1 + A_{2CBO} cos(2\omega_{CBO}(t) + \phi_{2CBO}) e^{-\frac{t}{2\tau_{CBO}}} \\
N_{VW}(t) &= 1 + A_{VW} cos()\omega_{VW}(t) + \phi_{VW} e^{-\frac{t}{\tau_{VW}}} e^{-\frac{t}{\tau_{VW}}} \\
N_y(t) &= 1 + A_y cos(\omega_y(t)\, t + \phi_y) e^{-\frac{t}{\tau_y}} \\
\Lambda(t) &= 1 - k_{LM} \int_{t_0}^{t} e^{\frac{t'}{\gamma\tau}} L(t') dt'
\end{aligned}
$$

Where N_{CBO} is the effect of the first harmonic of the coherent betatron oscillation, N_{2CBO} is the effect of the second harmonic of the CBO, N_{VW} is the effect of the vertical waist, N_y is the effect of the oscillation in the vertical plane and Λ is the effect of lost muons.

Fit procedure

The 22 parameters fit doesn't converge unless all the parameters are initialized in a range around their true value. The fit procedure consists in several steps, starting from the simplest model with only 5 parameters, then progressively adding parameters to account for peaks in the residuals Fourier transform. Once the the best-fit parameters for the 5 parameters

1. First the 5 parameters function is fitted
2. A function with more parameters is considered, all the parameters determined in the previous step are fixed
3. The function is fitted to determined the values of the free parameters
4. all parameters are released, the function is fitted again initializing the parameters to the values found at the previous step
5. this procedure is repeated until all parameters are included

The fit is done using the χ^2 minimization algorithm included in the TMinuit2 package in ROOT.

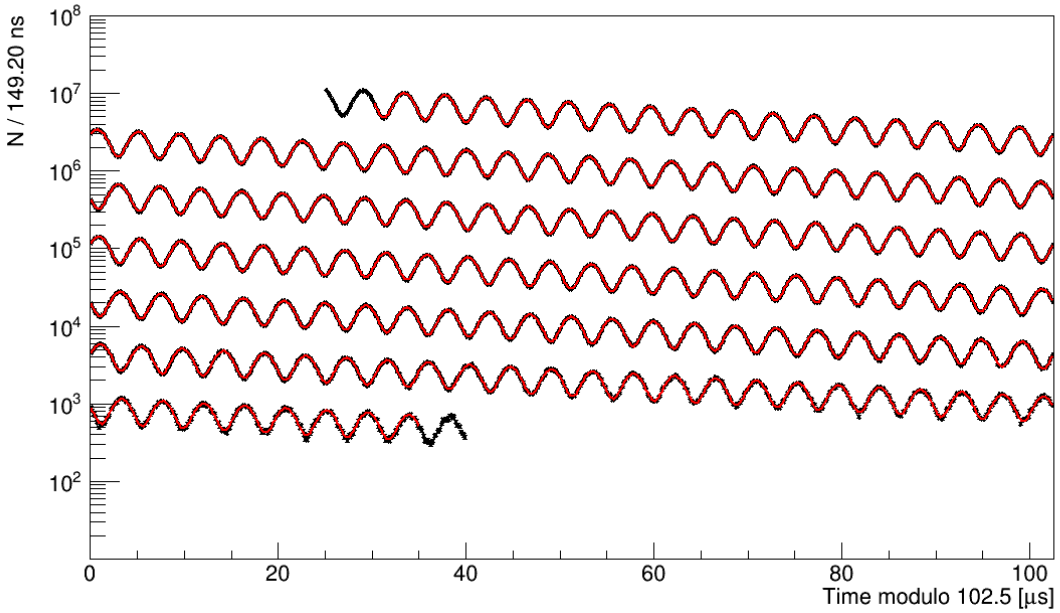

Figure 3.8: Fitted wiggle plot where the time axis is wrapped on itself.

Chapter 4

T and A methods comparison

The two method gives the following results: As we can see from 4.1 the A-method uncertainty

	R (ppm)	δR (ppm)	χ^2/ndf	χ^2/ndf
T-method	-81.709	0.701	4297.19/4133	1.039
A-method	-81.429	0.631	4364.88/4133	1.056

Table 4.1: T and A method comparison

is 10% lower than the T-method uncertainty, which is compatible with a $10\% - 20\%$ improvement that we expect. The A-method has a slightly higher χ^2 but this is also expected because the A-method uses more statistics. The agreement between the two method is checked by calculating the difference:

$$|R_T - R_A| = 0.280 \tag{4.1}$$

this difference should be lower than the allowed statistical deviation, which is the 1σ difference due to different amount of statistics. The allowed statistical deviation is defined as:

$$\sqrt{\delta R_T^2 + \delta R_A^2 - 2r\delta R_T \delta R_A} \tag{4.2}$$

where r is the correlation between the two methods. In first approximation we can assume maximum correlation $r = \sigma R_A / \sigma R_T$, which turns the equation 4.2 in to:

$$\sqrt{\delta R_T^2 - \delta R_A^2} = 0.305 \tag{4.3}$$

with this assumption the results are compatible.

4.1 T and A method correlation

The two methods are not independent because part of the data is shared. The correlation factor r can be estimated using many independent measurement of R, measurement are obtained from pseudoexperiments generated with the bootstrap method. In this analysis two approaches were used.

Pseudoexperiments from 2D histogram

We generate pseudoexperiments extracting random entries from the pile-up corrected energy-time distribution, each time with a different seed, for a total of 2000 pseudoexperiments. For each of them we build the wiggle plot using both T and A methods, that are then fitted with the 22 parameters function. The values of R obtained from the fit are used to estimate the correlation factor. In 11 cases the fit didn't properly converge, as the parameter R had a very

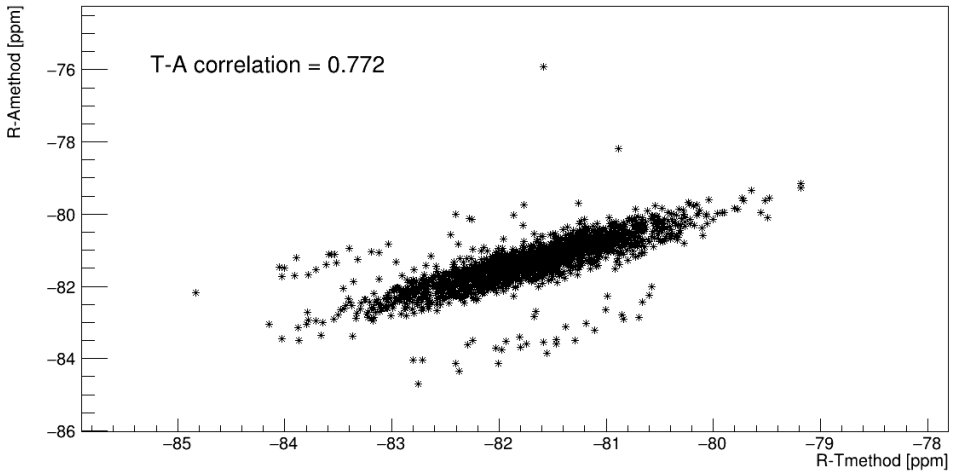

Figure 4.1: Scatter plot of R_A vs R_T from the 2D histogram.

high uncertainty, these points are excluded from the calculation. Now we can calculate the correlation factor by plotting the values of R on a scatter plot: the result is $r = 0.772$, which is lower than the one obtained in Run 1 $r = 0.905$. This suggests that this method mat not be accurate enough.

Pseudoexperiments from 1D histograms

Another approach is to build pseudoexperiments from the 1D wiggle plot. We fill every bin with a number of entries that is randomly extracted from a Poisson distribution with mean equal to the number of entries of the original wiggle plot. The error on each bin is calculated as:

$$error_{bootstrap} = error_{OG} \times \frac{entries_{bootstrap}}{entries_{OG}} \tag{4.4}$$

that means the error of the bin of the original plot multiplied by the ration of the entries. This method has the advantage of greatly reducing the computational time. Again, after fitting

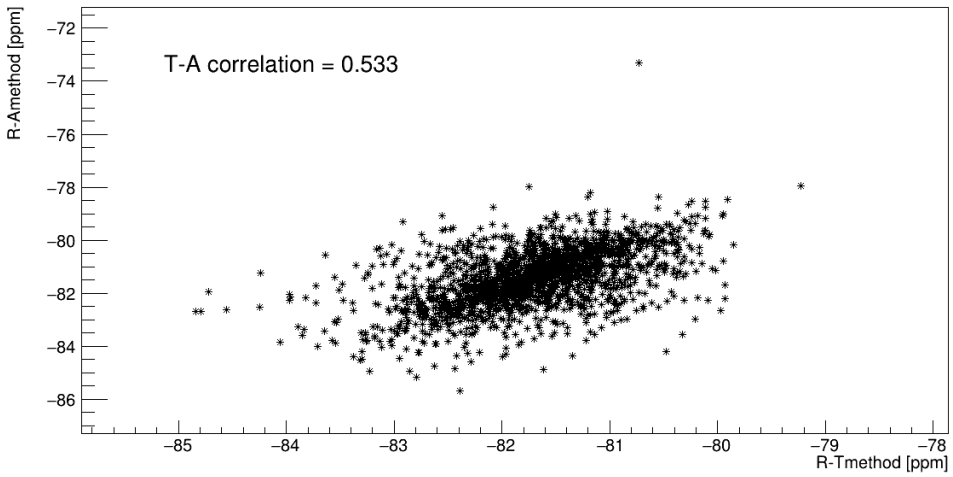

Figure 4.2: Scatter plot of R_A vs R_T from the 1D histogram with entries extracted from a Poisson distribution.

each wiggle plot with the 22 parameters function, the values of R are plotted on a scatter plot. With this method the correlation factor is estimated to be $r = 0.533$, even lower than before.

The final attempt is to extract entries from a Gaussian distribution instead of a Poisson distribution. Repeating the procedure and drawing the scatter plot, we see that the points align on 3 lines. Indeed, plotting the distribution of the difference $R_T - R_A$ highlights that

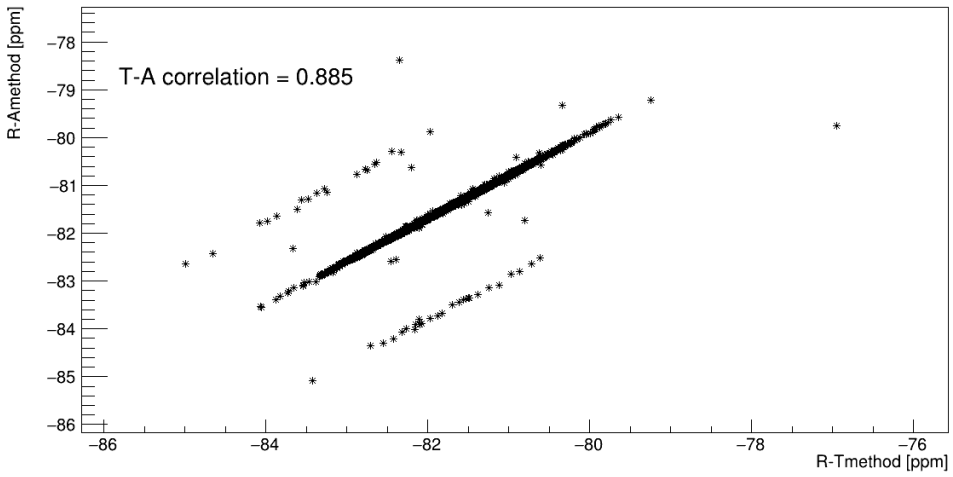

Figure 4.3: Scatter plot of R_A vs R_T from the 1D histogram with entries extracted from a Gaussian distribution.

some point have almost a fixed difference. This effect could be due to the random number generator algorithm. We correct for this effect by removing points that have a difference

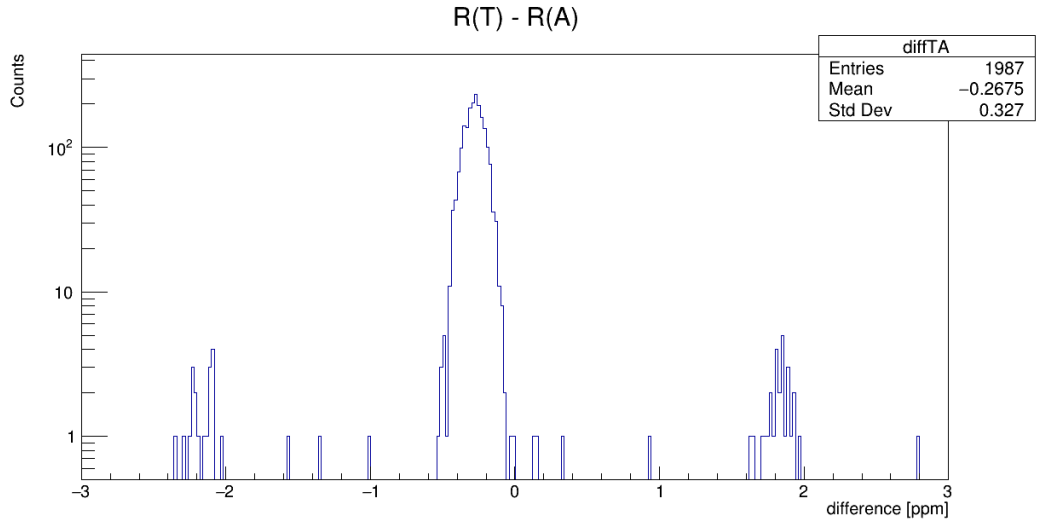

Figure 4.4: Distribution of the difference $R_T - R_A$, we can see that while the majority is centered around zero, while some points fall at -2 or 2.

greater than 1, this correction removes 13 points. From the scatter plot in figure 4.5 the

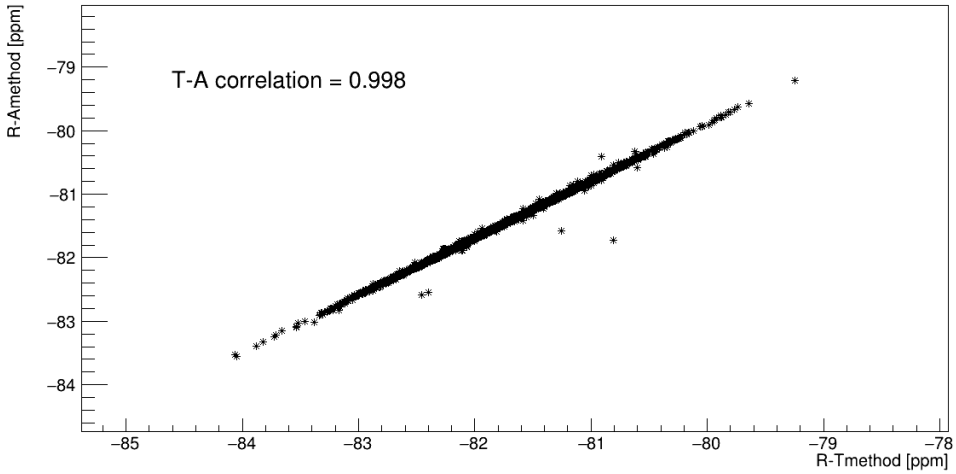

Figure 4.5: Scatter plot of R_A vs R_T from the 1D histogram with entries extracted from a Gaussian distribution.

correlation factor between the two methods is $r = 0.998$, and the allowed statistical deviation is 0.081.

Conclusions

During these two months at Fermilab I had the opportunity to learn about the goal and specifics of the E989 experiment. I was able to reproduce the fit procedure used for Run1 on data from Run2, obtaining the blinded anomalous precession frequency. I also learned a lot about the bootstrap method and random number generation while studying the correlation between the T and A methods.

My thanks go to my supervisors Prof. Brendan Casey and Prof. Marco Incagli, and to Matteo Sorbara, Alberto Lusiani, Paolo Girotti and Anna Driutti, for the extensive help and knowledge that they gave me.

REFERENCES

- B. Abi et al. (Muon g -2 Collaboration) – Measurement of the Positive Muon Anomalous Magnetic Moment to 0.46 ppm Phys. Rev. Lett. 126, 141801 (April 2021)
- T. Albahri et al. (Muon g-2 Collaboration) – Measurement of the anomalous precession frequency of the muon in the Fermilab Muon g-2 Experiment Phys. Rev. D 103, 072002 (April 2021)
- M. Sorbara – Measurement of the Anomalous Precession Frequency in the Muon g-2 Experiment at Fermilab PhD. Thesis (March 2022)